PERGAMON

Engineering Failure Analysis 6 (1999) 267–276

ENGINEERING FAILURE ANALYSIS

Failure analysis of counter shafts of a centrifugal pump

G. Das*, A.N. Sinha, S.K. Mishra (Pathak), D.K. Bhattacharya

National Metallurgical Laboratory, Jamshedpur 831 007, India

Received 14 August 1998; accepted 12 September 1998

Abstract

An analysis of the premature failure of two counter shafts used in centrifugal pumps for lifting slurry has been carried out. Chemical analysis, microstructural characterisation, fractography, hardness measurement, tensile and Charpy impact tests were used for the analysis. The chemical compositions for the shafts were as per recommendation. The microstructure of one of the shafts was ferritic–pearlitic and its mechanical properties were inferior to the recommended values. For the other shaft the microstructure was tempered bainite; although the impact energy satisfied the specification, the other properties (hardness, UTS) were inferior. It was concluded that the improper heat treatment was the prime cause for the premature failure of the shafts.

Keywords: Fatigue; Heat treatment; Machinery failures; Shafts

1. Introduction

A shaft is a metal bar usually cylindrical in shape (solid or hollow), used to support rotating components or to transmit power or motion by rotary or axial movement. Shafts operate under a broad range of service conditions including various corrosive environments and a wide temperature range. Shafts may be subjected to a variety of loads such as tension, torsion, compression, bending or a combination of these. Shafts are also sometimes subjected to vibratory stress [1, 2].

Shafts are made of various materials according to their applications and requirements. EN24 (AISI/SAE4340) steel is one of the common shaft materials. This is a medium carbon, low alloy steel. It is used where high strength and toughness are required for thick sections. It combines deep hardenability with ductility, toughness and strength [3, 4]. It also has good fatigue resistance. This steel can be case hardened without difficulty and finds many applications [5]. Its properties can be tailored by varying heat treatment schedules to get a good combination of mechanical properties and microstructure [6, 7]. Hardening can be done by oil quenching (up to 75 mm diameter) or by water quenching (for larger sections) [8]. After hardening by either process, tempering is carried

* Corresponding author. Tel.: +91 657 426091; fax: +91 657 426527; e-mail: gd@csnml.ren.nic.in

1350-6307/99/$ - see front matter
PII: S1350-6307(98)00037-5

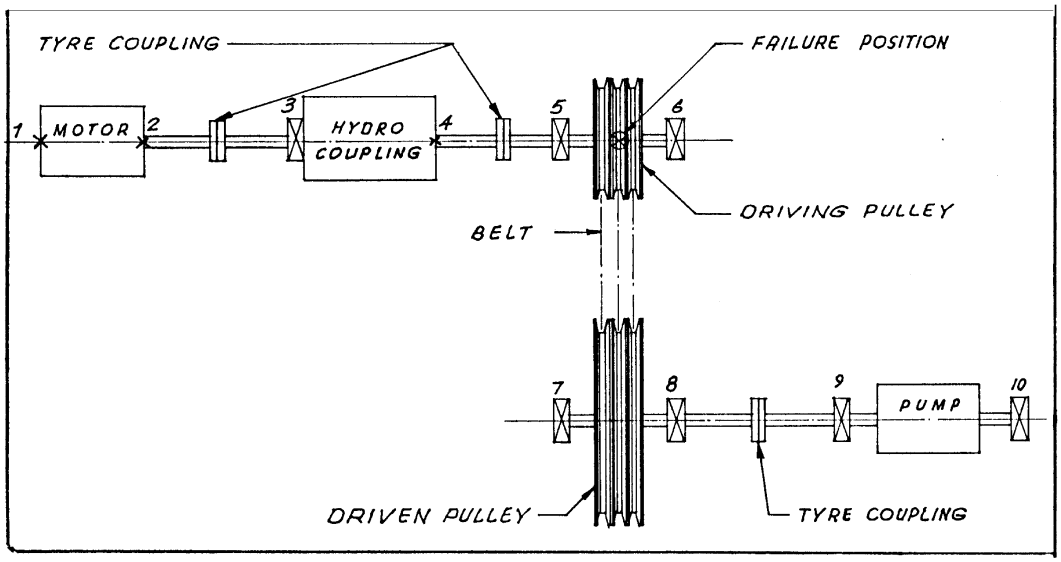

Fig. 1. Schematic diagram of the failed centrifugal pump.

out to reduce internal stresses and to optimise mechanical properties. Impact energy is one of several mechanical properties which is governed by the tempering treatment. It has been found that impact toughness may differ for various microstructures though their hardness value may be kept at a specific level [9].

This paper presents the analysis of failure of two EN-24 shafts used in centrifugal pumps for lifting slurries in a power plant. The failed shafts were made of EN24 steel. The shafts were of 6 cm (shaft A) and 7 cm (shaft B) diameter and were required to work for at least three years of continuous operation. Shaft A failed only after 16 days and shaft B after 10 days of operation. A schematic diagram of the entire pump is shown in Fig. 1 and the location of fracture is indicated by arrow marks. For both the cases, the breakage of the shafts was found to be in the centre of the pulley. The tensions of the belts were given as per the recommendation of the belt manufacturer. Prior to failure, no abnormal vibration was observed in the bearings associated with the shafts. Also after the shaft failure, the bearings were found to be in good condition. In Fig. 1 the motor, hydro-coupling and bearings 5 and 6 are mounted on one base whereas bearings, 7 and 8 and the pump are mounted on a separate base.

2. Experimental procedure

The microstructure of the shaft material was analysed by optical microscopes and a JEOL 840 scanning electron microscope (SEM) equipped with an energy dispersive X-ray (EDX) analysis facility. The composition of the shaft material was determined by using a standard spectrometer analyser as well as by using SEM–EDX. The samples for microstructural studies were prepared in the usual metallographic manner both in the transverse and longitudinal direction of the shaft axis. They were polished and etched with 5% nital (nitric acid in ethanol). Fractography of the

broken shafts was carried out by SEM. Hardness testing was performed using a Vickers Hardness testing machine under 30 kg load. Tensile tests were carried out on cylindrical specimens as per ASTM standards by using a servo hydraulic INSTRON machine. Standard sized specimens for Charpy impact tests were made in longitudinal and transverse directions from both the shafts. The specimens were then tested in a Wolpert instrumented impact testing machine using 100 and 150 J hammers to get impact toughness values.

3. Results

3.1. Visual examination

Visual examination of the failed end gave the appearance that both the shafts failed by fatigue. A macroscopic view of the failed region of shaft B is shown in Fig. 2. Signs of smearing and distortion at the key edge were observed. Both the shafts failed at the end where the pulley is fitted as shown by the arrow mark in Fig. 1.

3.2. Chemical analysis

The chemical analyses for both shafts A and B are listed in Table 1. SEM–EDX analysis also showed a similar composition for both shafts. It confirmed that they were made of EN24 steel.

3.3. Microstructural analysis

Figure 3 shows the representative microstructures in the longitudinal direction for shafts A and B. The microstructure in the transverse direction was essentially the same. The microstructure is

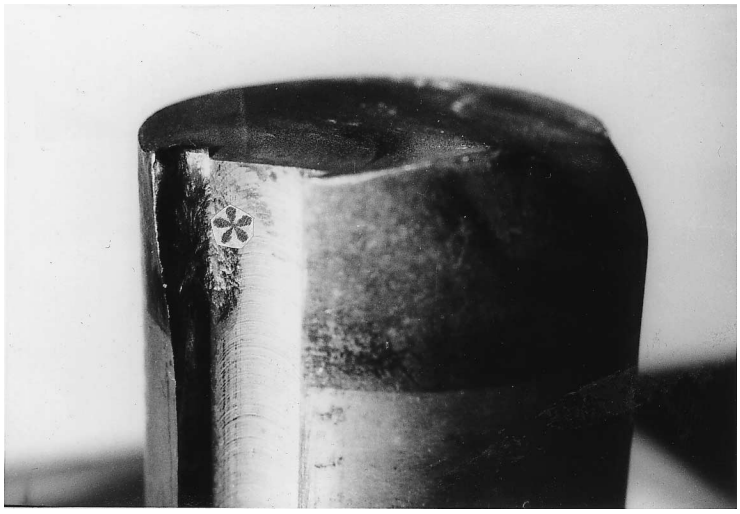

Fig. 2. Macroscopic view of failed end of shaft B.

Table 1
Chemical analysis for shaft material

Shaft	C	Si	Mn	S	P	Ni	Cr	Mo
A	0.41	0.25	0.47	—	—	0.97	0.99	0.12
B	0.44	0.20	0.43	—	—	0.96	0.85	0.22

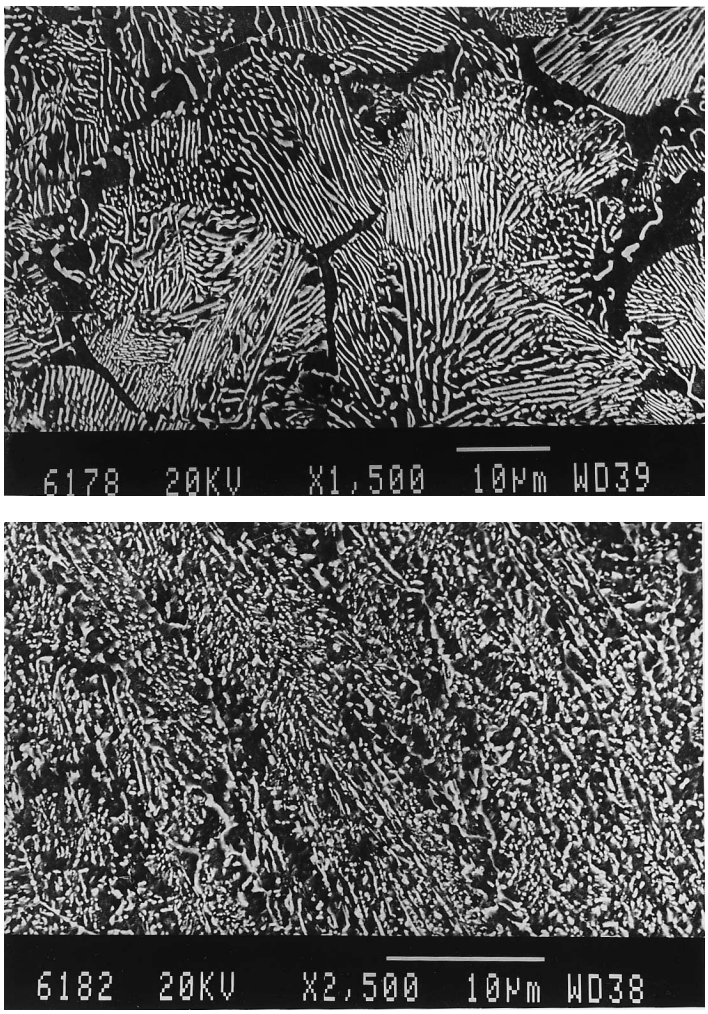

Fig. 3. SEM micrograph of (a) shaft A, showing ferritic–pearlitic microstructure and (b) shaft B, showing tempered bainitic microstructure.

observed as ferrite–pearlite for shaft A (Fig. 3(a)). Black patches indicate ferrite in the microstructure. A tempered bainitic microstructure was observed for shaft B, shown in Fig. 3(b). No significant inclusions or segregations were found; only a few pores were observed on the polished surface. The presence of pores are below the level of concern. The material used for the machining of the shafts was almost clean, only a few oxide inclusions of D4 fine ratings were observed.

Figure 4 shows the microstructure of the distorted region along the axis and along the transverse direction at the key region (indicated by * in Fig. 2) of shaft B. Lapping of thin layers and some smearing of metal was found near the key region (Fig. 4(a)). Microstructural analysis of Fig. 4(b) indicated the presence of plastic flow lines. It is also observed that the cracks had initiated from the smeared region (Fig. 4(b)).

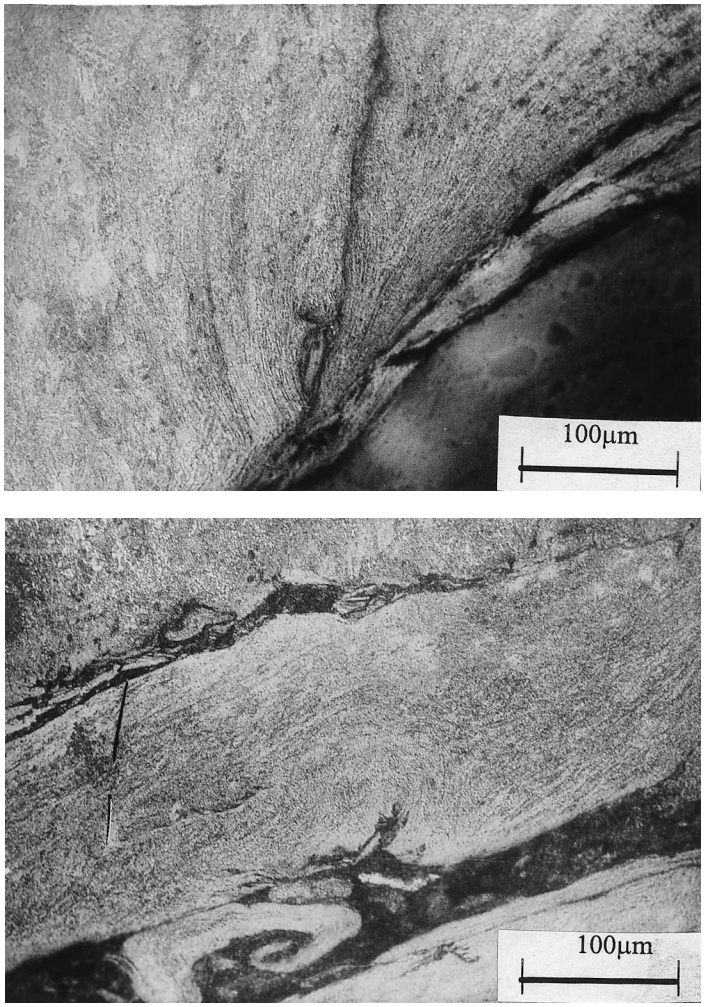

Fig. 4. Optical micrographs for shaft B at key region (marked by * in Fig. 2) (a) along the axis and (b) along the transverse direction.

3.4. Fractography

An SEM fractograph for shaft A is shown in Fig. 5. The fracture surface of the broken shaft showed that the fracture was by fatigue (Fig. 5(a)) and the cracks initiated from the locking key sites. The apparent striations observed in Fig. 5(b) are actually likely to be fractured pearlite. Figure 5(c) shows that the cracks had initiated from the keyway region. Propagation of secondary cracks was also observed, as shown in Fig. 5(d). A cavity of size approximately 300–400 μm was observed in the fracture surface.

Similarly shaft B also failed by fatigue. The presence of striations in Fig. 6 supports the view of fatigue failure. Here also, the crack had initiated from the distorted key region where some plastic flow of metal was observed.

3.5. Mechanical testing

3.5.1. Tensile

Cylindrical specimens for tensile tests were prepared from shaft B along the longitudinal direction. The test was performed with a strain rate of 10^{-3}/s. The stress–strain diagram is shown in Fig. 7. The yield strength, UTS and % elongation were found to be 530, 750 MPa and 22.55 respectively. The YS and UTS values were below the recommended level whereas % elongation satisfied the requirement.

3.5.2. Impact

The results of the impact tests along the longitudinal and transverse directions are given in Table 2.

3.5.3. Hardness

Hardness values were obtained from the curved surface, as well as from the transverse cut surface. A number of readings at various locations across the cross section of the shafts were taken in order to determine the variation of hardness, if any. No appreciable variation in the hardness values was detected across the cross section. The average hardness values for shafts A and B were 170 and 240 HV respectively.

4. Discussion

4.1. Shaft A

Chemical analysis showed that the shaft was made of EN24 steel which is a recommended material for such applications. The shaft was of a ferritic–pearlite nature, whereas for this type of shaft the final microstructure should be tempered martensite [5]. Proper tempering should be done after solution followed by oil quenching and rough machining. The impact energy obtained was far lower than the specified level. The hardness value was found to be 170 HV, which is also lower than the recommended value for such applications. According to specification, the hardness value should be 340–400 HV [4, 5]. Visual examination and fractographic study of the failed shaft

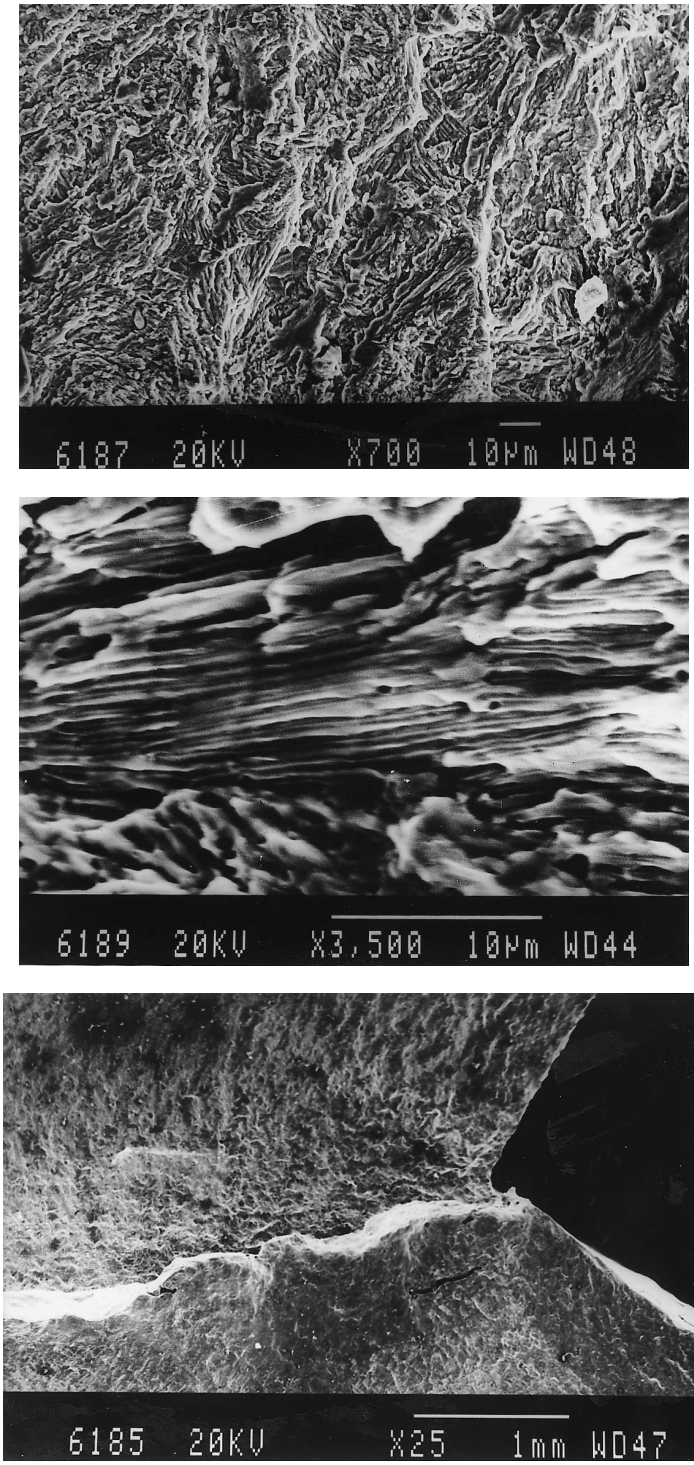

Fig. 5. SEM fractograph for shaft A showing (a) fatigue failure, (b) apparent striations, (c) crack initiation region and (d) secondary cracks.

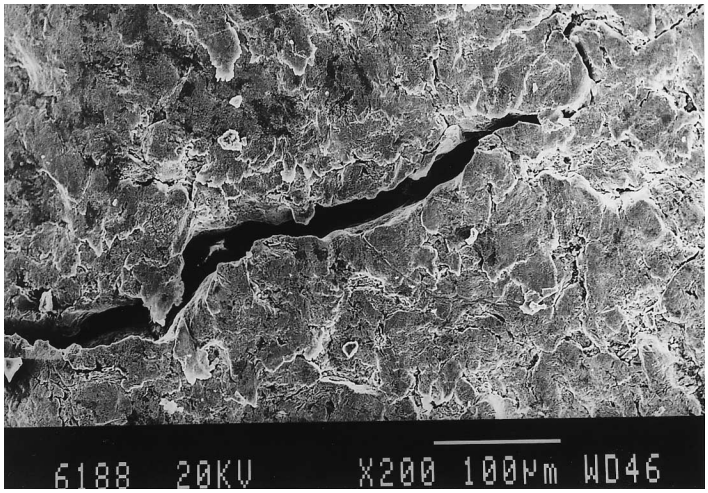

Fig. 5. (*continued*)

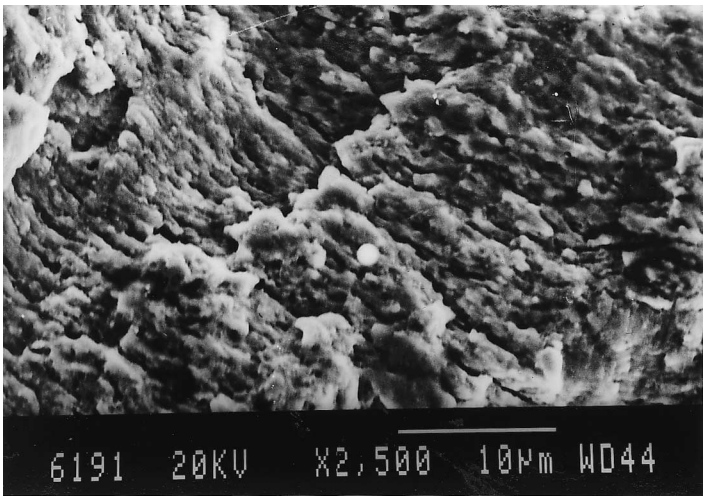

Fig. 6. SEM fractograph for shaft B showing fatigue striations.

disclosed that cracks had propagated from one of the keyways and failure was by fatigue. From the above discussions, it is clear that the heat treatment of the shaft was not properly done.

4.2. Shaft B

Shaft B was also made of EN24 steel, confirmed by chemical analysis. The microstructure was predominantly tempered bainite. The hardness value was found to be 240 HV, still below the recommended level, while the impact energy was as per recommendation (51 J) [4, 5]. Though the

Table 2
Impact energy for both shafts

Shaft	Specimen direction	Impact energy	
		J	ft lbf
A	Longitudinal	17.5	12.96
	Transverse	15.5	11.1
B	Longitudinal	51	37.78
	Transverse	23	17

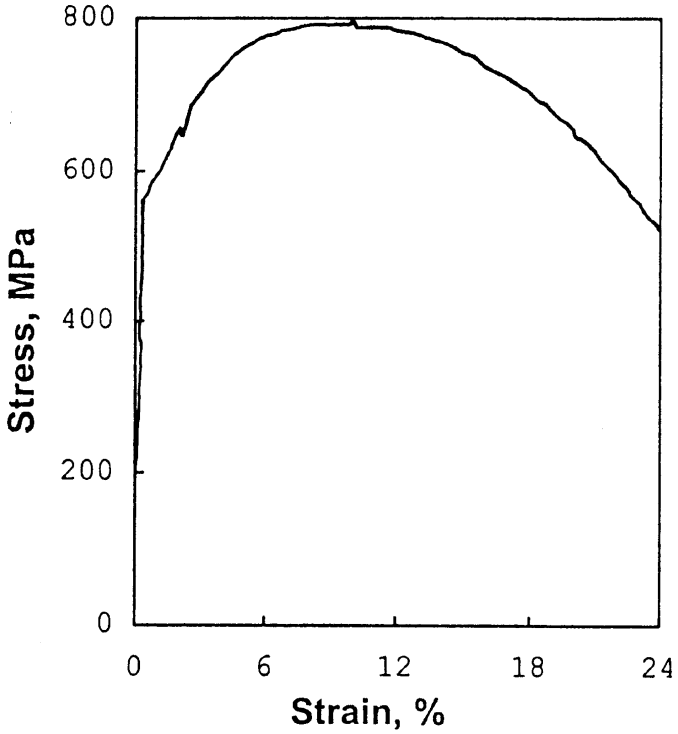

Fig. 7. Stress–strain diagram for shaft B.

impact value satisfied the requirement for the present application, there was a lack of hardness and strength which might be a prime cause for the ultimate failure of shaft B.

Again, one of the keyways near the fracture surface was heavily deformed. Visual as well as microscopic analysis of the fracture shaft disclosed that the crack had initiated from the distorted region, shown in Fig. 1. Analysis of SEM fractographs confirmed the above. The microstructure of the plastically deformed region shows (Fig. 6) that the crack originated from the deformed region and propagated radially towards the centre. Here pulleys were assembled on the shaft by

means of shrink fitting, which resulted in a stress raiser under bending stress. Improper fitting may also result in friction between the shaft and the pulley. Friction produces wear of the shaft, resulting in wear induced surface roughness and fretting, all of which might promote nucleation and growth of cracks. Friction can also activate metal flow as a result of plastic deformation.

5. Conclusions

The shafts (consisting of ferrite–pearlite for A and tempered bainite for B) were made of EN24 steel. The materials did not show significant inclusions or segregation. Only a few pores were noticed on the polished surfaces. Fractography observations revealed the signature of fatigue failure for both cases. The mechanical properties of the shaft materials were found to be inferior, though the impact energy for shaft B satisfied the requirements. Cracks were found to have originated from the key area of the shaft. For shaft A, improper heat treatment produced an undesirable microstructure and thus resulted in a low CVN toughness and low hardness of the shaft material. This was the primary cause of failure. For shaft B improper heat treatment resulted in low values of strength and hardness which made the material more prone to failure. Again, the shaft and pulley were not properly fitted, which led to fretting between the two components and aggravated the failure mechanism.

Acknowledgements

The authors would like to thank Mr S. Das and Dr S. Ghosh Choudhary, for their help and many stimulating discussions. They are also grateful to Prof. P. Ramachandra Rao for encouragement and permission to publish this work.

References

[1] Shaikh H, Kathak HS, Gnanamoorthy JB. Analysis of service water pump shaft failure. Prakt. Meta., 1990:27(7):362.
[2] Fraccis P. Shaft failure. Some common causes. Mach. Prod. Eng., 1974:124:195.
[3] Woolman J, Mottrum RA. The mechanical and physical properties of the British Standard EN Steel, vol. 2. Pergamon Press, Oxford, 1966.
[4] Agarwal V. Steel handbook. Gandhinagar: Vishwas Techno-Publishers, 1990.
[5] Metal handbook, failure analysis and prevention, vol. 11, 9th ed. ASM, 1986.
[6] Tomita Y. J. Mat. Sci., 1992;27(7):1705.
[7] Tomita Y. J. Mat. Sci., 1989;24(4):1357.
[8] Heat treater's guide, practice and procedure for iron and steels, 2nd ed. ASM International, 1995.
[9] Singh SR et al., editors. Proceedings of the clinic on failure analysis. India: NML, 1997.